The Korean Journal of Ceramics, **6**[2] 177-182 (2000)

Variation of Oxygen Nonstoichiometry of Porous $La_{0.6}Ca_{0.4}MnO_{3-\delta}$ SOFC-Cathode under Polarization

Junichiro Mizusaki, Hideki Narita,* Naoya Mori, Masayuki Dokiya and Hiroaki Tagawa*****

Research Institute for Scientific Measurements, Tohoku University, 2-1-1 Katahira, Aoba-ku, Sendai, 980-8577, Japan
Institute of Environmental Science and Technology, Yokohama National University, Tokiwadai, Hodogaya-ku, Yokohama, 240-8501, Japan
** Now with Akebono Brake R & D Center, 5-4-71 Higashi, Hanyuu-shi, Saitama, 348-8501 Japan*
***Now with Murata Co. Ltd., Yasu-gun, Shiga, 520-23, Japan*
****Deceased*

(Received September 23, 1998)

At the porous $La_{0.6}Ca_{0.4}MnO_{3-\delta}$ (LCM)/YSZ electrodes of solid oxide fuel cells (SOFC), the electrochemical redox reaction of oxygen proceeds via the triple phase boundary (TPB) of gas/LCM/YSZ. The surface diffusion of adsorbed oxygen on LCM has been proposed as the rate determining process, assuming the gradient of oxygen chemical potential from the outer surface of porous layer to TPB. Along with the formation of this gradient, oxygen nonstoichiometry in the bulk of LCM may varies. In this paper, an electrochemical technique was described precisely to determine the variation of oxygen content in LCM of porous LCM/YSZ under polarization. It was shown that the oxygen potential in LCM layer under large cathodic polarization is much lower than that in the gas phase, being determined from the electrode potential and Nernst equation.

Key words: Nonstoichiometry, SOFC, Cathode, Electrode reaction, $La_{0.6}Ca_{0.4}MnO_3$, Solid electrolyte, Perovskite-type oxide

I. Introduction

1. Purpose

High temperature operation of as high as 1000°C has been considered for the solid oxide fuel cells (SOFC) for large scale power stations. In such SOFC systems, perovskite-type manganites, $La_{1-x}AE_xMnO_{3-\delta}$ (AE=Sr, Ca) have been considered as the best materials for cathode because of their high chemical and thermal compatibility with YSZ electrolytes. In order to reduce the cathode overpotential, the structure of the oxide electrode must be optimized to enhance the electrode reaction rate. To elucidate the optimum structure, the knowledge on the electrode reaction mechanisms vitally important, such as the microscopic sites at which the rate determining reaction takes place and the process how the variation in the micro-structure affects the kinetics.

In the past decade, the author and co-investigators have studied the mechanism of the electrode reaction at the air electrodes of solid oxide fuel cells, mostly using $La_{0.6}Ca_{0.4}MnO_3$/YSZ as a typical example. Based on our preceding studies of the present authors summarized below, the research in this paper is focused on the confirmation of oxygen nonstoichiometry variation in the oxide cathode due to the electrochemical polarization.

2. Outline of the Preceding Works on the Electrode Reaction Path

So far, the authors have studied the electrochemical impedance and the current-overpotential relationships on the porous $La_{0.6}Ca_{0.4}MnO_3$/YSZ electrode system in air as a function of electrode thickness,[1] as to the variation with microstructures,[1,2] and as to the dependence on $P(O_2)$ and temperatures.[3] It was shown that the predominant reaction path is through the triple phase boundary (TPB) consisting of the gas phase, $La_{0.6}Ca_{0.4}MnO_3$, and YSZ,[1] and the reaction rate is essentially proportional to the length of TPB.[2] The steady-state polarization current, i, under the overpotentials, η, within ±150 mV was found to be approximately expressed by[3]

$$i = kP(O_2)^{1/2}[\exp\{2F\eta/(RT)\} - \exp\{-2F\eta/(RT)\}] \quad (1)$$

where k is the rate constant, $P(O_2)$ is the gas phase oxygen partial pressure in the unit of 10^5 Pa. It was also reported that limiting current was observed for η<-150 mV, at which the current is proportional to $P(O_2)$.

The overpotential η is determined by the difference in the oxygen chemical potential, μ_O, in YSZ at the $La_{0.6}Ca_{0.4}MnO_3$/YSZ interface at equilibrium and under the proceedings of the reaction. Here, μ_O is related to the oxygen activity, a_O, in YSZ adjoining the electrode by

$$\mu_O = RT \ln a_O \quad (2)$$

At equilibrium, $a_O^2 = P(O_2)$. Then, we have

$$\eta = 1/(2F)\ RT \ln [a_O/P(O_2)^{1/2}] \quad (3)$$

and Eq. (1) is expressed by

$$i=k[a_O-P(O_2)a_O^{-1}] \quad (4)$$

This electrode reaction can be expressed in a style of chemical reaction as shown in Eq. (4), and the rate determining reaction process does not involve the electron exchange between $La_{0.6}Ca_{0.4}MnO_3$ and YSZ, but rather a chemical one.

Recently, using porous $La_{0.8}Sr_{0.2}MnO_3$ instead of $La_{0.6}Ca_{0.4}MnO_3$, Kamata found that the rate determining process varies with the electrode morphology and the surface diffusion of adsorbed oxygen on the electrode from the outer surface to TPB is one of the predominant rate determining process.[4,5] The rate equation for the surface diffusion controlled kinetics in the complete form is complicated.[4-6] However, under ordinary conditions at which the coverage of adsorbed oxygen on the surface is much lower than 0.5, the rate equation can be simplified to

$$i=k[a_O-P(O_2)^{1/2}] \quad (5)$$

The contribution of oxide ion diffusion in the bulk of the oxide electrode material has been investigated by Hammouche *et al.*[7] and the present authors.[8] When the electrode is porous, the bulk diffusion becomes obvious only under large cathodic overpotentials of nearly 1 V.[7] By using a dense $La_{0.63}Sr_{0.27}MnO_3$ electrode prepared on partially stabilized zirconia, the authors tried to limit the reaction path only to the bulk diffusion. The reaction rate by the bulk diffusion was found to be expressed by

$$i=(2FL)^{-1}\int_{\mu(O)=\mu(O,0)}^{\mu(O,L)}\sigma(O^{2-})d\mu_O \quad (6)$$

Here, the positions of the gas/oxide electrode interface and the dense oxide electrode/electrolyte interface are denoted by 0 and L, respectively. Since oxygen vacancy concentration in $La_{1-x}AE_xMnO_3$ in air and other oxygen rich atmospheres is very small,[9] the oxide vacancy concentration, hence $\sigma(O^{2-})$, depends on $P(O_2)^{-1/2}$. Then, the current by the bulk diffusion of oxide ion through the electrode is expressed by

$$i=k[P(O_2)^{-1/2}-a_O^{-1}] \quad (7)$$

Due to the very small $\sigma(O^{2-})$, the current through the bulk diffusion is much smaller than that via TPB in the usual cathode $P(O_2)$ conditions.

The reaction path related to Eqs. (4), (5), and (7) are schematically shown in Fig. 1. These reactions are considered to take place in parallel. The driving force is the difference in the oxygen chemical potential between the gas phase and the $La_{0.6}Ca_{0.4}MnO_3$/YSZ interface. Then, the oxygen chemical potential in $La_{0.6}Ca_{0.4}MnO_3$ must deviate from that of the gas phase. The schematic profile of oxygen chemical potential considered in the gas/$La_{0.6}Ca_{0.4}MnO_3$/YSZ system under cathodic polarization is shown in Fig. 2. Since $La_{0.6}Ca_{0.4}MnO_3$ shows some extent of oxygen nonstoichiometry, the change in chemical potential may accompany the change in the oxygen content of $La_{0.6}Ca_{0.4}MnO_3$ electrode.

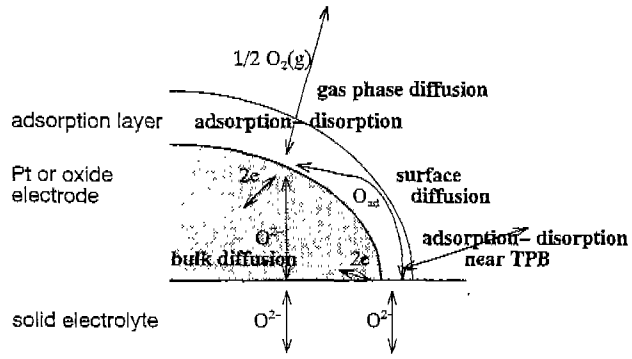

Fig. 1. Reaction path considered for the oxide cathode of SOFC.

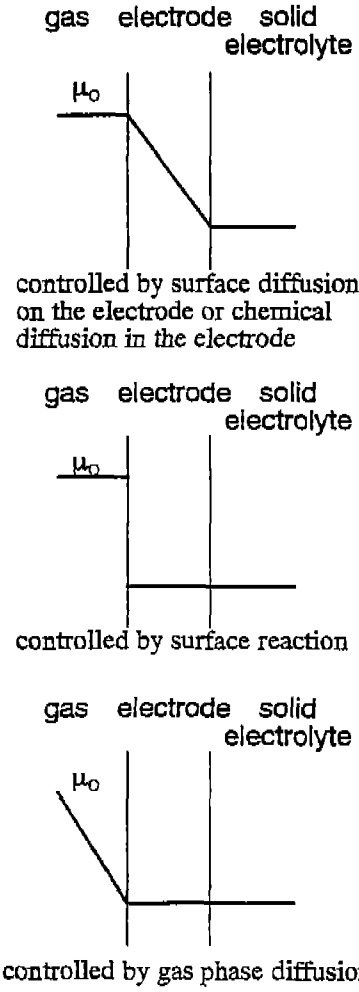

Fig. 2. Schematic oxygen chemical potential profiles in the oxide cathode of SOFC.

That is, when the cathodic overpotential is applied, oxygen may be released from the $La_{0.6}Ca_{0.4}MnO_3$ layer, and when the cathodic current is interrupted, the oxygen may be absorbed by $La_{0.6}Ca_{0.4}MnO_3$ to retain the equilibrium with the gas phase.

3. Oxygen Evolution and Incorporation due to Nons-

toichiometric Variation of Oxygen in the $La_{0.6}Ca_{0.4}MnO_{3-\delta}$ Cathode during the Polarization.

The authors and their co-investigators have already found the oxygen evolution and incorporation of $La_{0.6}Ca_{0.4}MnO_3$ cathode accompanying the variation of overpotential, and reported the related phenomena in part in several proceedings[10,11] and papers:[12,13] In the proceeding papers, the excess oxygen evolution or incorporation associating to the variation of overpotential was reported for the first as an anomaly, and the phenomena was interpretated in relation to the oxygen nonstoichiometry variation of the electrode materials.[10] Then, reported was the relationship of the phenomena to the contribution of oxide ion diffusion in $La_{0.6}Ca_{0.4}MnO_3$.[11]

When the variation of oxygen nonstoichiometry takes place at the counter electrode of $La_{0.6}Ca_{0.4}MnO_3$, the impedance spectra for the working electrode, either Pt or $La_{0.6}Ca_{0.4}MnO_3$, apparently indicate components of negative resistivity or reactance at low frequency.[12] From the standpoint of experimental technique of the electrode reaction kinetics, the measurement of excess oxygen evolution and incorporation was described and the relationship to the oxygen nonstoichiometry was briefly mentioned.[13]

Although the idea has been occasionally reported in part as shown above, the results are not yet published in a complete style. Moreover, in the preceding reports, some difference was seen in the oxygen nonstoichiometry by coulometric titration and by estimation from the oxygen evolution. In this paper, we summarize the experimental results and discussion on the oxygen nonstoichiometry in oxide electrode under polarization at the electrode system $La_{0.6}Ca_{0.4}MnO_{3-\delta}$/YSZ, using the nonstoichiometry of $La_{0.6}Ca_{0.4}MnO_3$ reevaluated by coulometric titration as well as high temperature gravimetry.

II. Experimental

1. Electrochemical Determination of Oxygen Evolution and Incorporation

The change in oxygen nonstoichiometry in $La_{0.6}Ca_{0.4}MnO_3$ under polarization was studied using the circuit shown in Fig. 3.[12] Disks of 8 m/oY_2O_3-ZrO_2 (YSZ), 10 mm in diameter and 3-5 mm in thickness, were prepared from the YSZ powder, NZP-D8Y (Nissan Chemical Industries, LTD), by uniaxial pressing with 4×10^6 g/cm^2 and sintering at 1400 °C. The density was more than 97%. Porous $La_{0.6}Ca_{0.4}MnO_3$ powder as WE was prepared by drip pyrolysis method and were mixed with turpentine oil, painted on YSZ fired at 1100°C for 2 h.[2] The disks was carefully weighed before and after mounting the porous $La_{0.6}Ca_{0.4}MnO_{3-\delta}$ layer, so that the amount of the $La_{0.6}Ca_{0.4}MnO_{3-\delta}$ layer applied to the cell was determined, which was 18-25 mg/cm^2 (=50-70 μm in thickness.)[1] Porous Pt as CE and RE was applied to YSZ pellet as shown in Fig. 4 by a similar way as described elsewhere.[2] The cell was placed in a gas stream of controlled $P(O_2)$ and flow rate of 100-105 cm^3/min. The oxygen content in the outlet gas was analyzed by a zirconia oxygen sensor of the type, sample gas, Pt/YSZ/Pt, air, kept at 750°C.

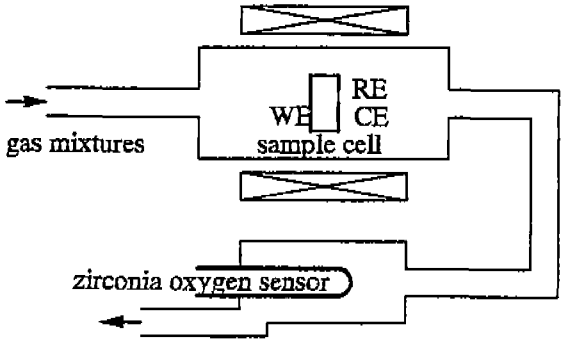

Fig. 3. Schematic setup of equipment for the measurements of nonstoichiometry change under cathodic polarization.

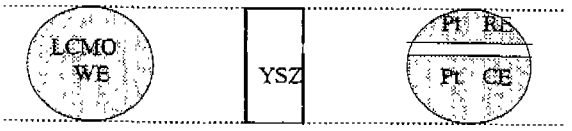

Fig. 4. Schematics of the electrode arrangement on the cell.

When current is applied, oxygen is incorporated to the cell at one electrode and released at another. Since all the electrodes are exposed to the same gas stream, when the nonstoichiometry in $La_{0.6}Ca_{0.4}MnO_{3-\delta}$ does not change with time, $P(O_2)$ of the outlet gas is the same to the inlet gas. The $P(O_2)$ deviation of the outlet gas from the inlet one indicates the change of δ in $La_{0.6}Ca_{0.4}MnO_{3-\delta}$.

Polarization studies were made at 800°C in the Ar-O_2 gas stream of $P(O_2)=10^2$, 10^3 Pa using a potentiostatic method, i.e., the potential between WE and RE was kept constant, E_{ap}. After the steady-state was attained, current was abruptly interrupted to determine the iR overpotential. In this paper, we use $P(O_2)=10^5$ Pa as the standard state of the electrode potential, E_{el}. That is, we calculated E_{el} from the observed potentials by the equation,

$$E_{el}=E_{ap}-iR+E_{eq} \quad (8)$$

Here, E_{eq} is the Nernst EMF between the gas phase $P(O_2)$ and $P(O_2) = 10^5$ Pa.

2. Determination of Nonstoichiometry by Static Methods

Nonstoichiometry of $La_{0.6}Ca_{0.4}MnO_{3-\delta}$ was measured as a function of $P(O_2)$ at 800°C in situ and in equilibrium conditions by using both a coulometric titration method and a high temperature gravimetry. Detailed procedures were described elsewhere.[14,15]

III. Results and Discussion

1. Oxygen Evolution and Incorporation

Fig. 5 shows a typical example of the relationship between the change of applied potential, E_{ap}, i and the EMF of the

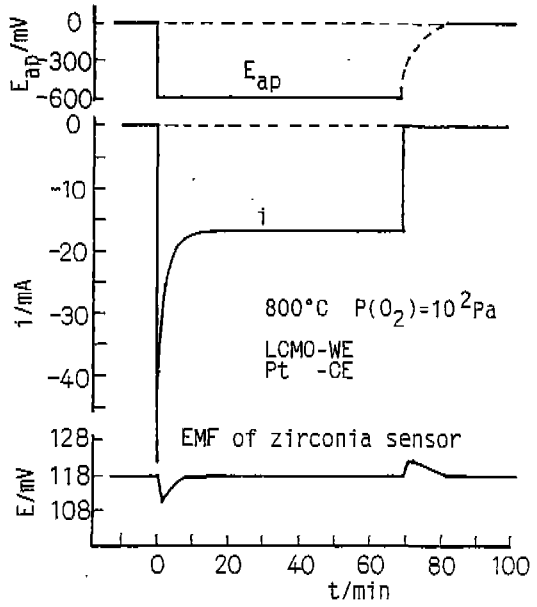

Fig. 5. Time change in the relationships among E_{ap}, i, and the EMF of oxygen sensor placed downstream of the cell.

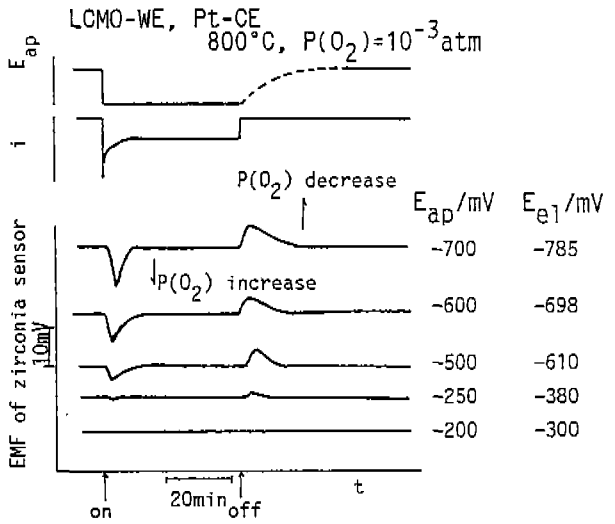

Fig. 6. Variation of the relationships in Fig. 5 with the applied potential. The steady state E_{el} is calculated from E_{ap} and Eq. (8).

zirconia sensor. The EMF change of the zirconia sensor indicates that the test cell releases oxygen at transient state of cathodic polarization, no excess oxygen evolution was observed under steady-state, and the cell incorporate oxygen when the current was interrupted.

Variation of this phenomena with the cathode overpotential is shown in Fig. 6. The electrode potential vs. $P(O_2)= 10^5$ Pa, E_{el}, is calculated using Eq. (8) and is also indicated, in the figure. The oxygen evolution and incorporation become remarkable for E_{el}>300 mV. Fig. 7 shows the polarization curve as a function of log i vs. E_{el} on which indicated was the region at which oxygen evolution and incorporation were observed. The region essentially overlaps the one at which limiting current is observed.[3]

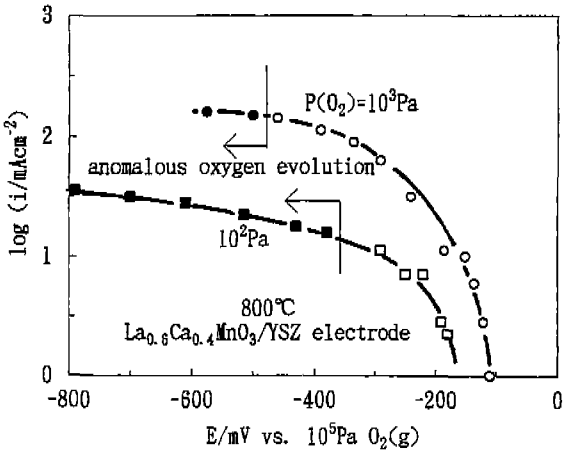

Fig. 7. Cathodic polarization curve on which the region is indicated at which obvious oxygen evolution and incorporation take place.

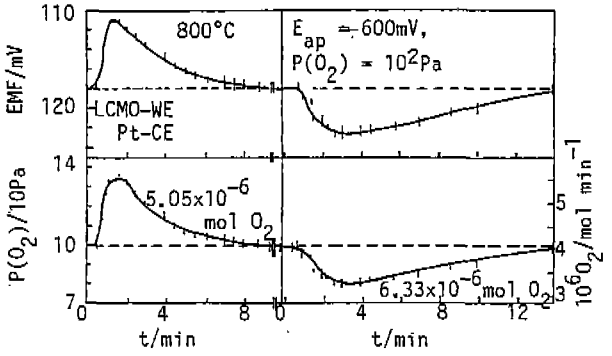

Fig 8. Calculation of oxygen evolution and incorporation by the electrode oxide from the EMF change of zirconia sensor.

Fig. 8 shows the procedure for the calculation of the amount of oxygen released or incorporated by $La_{0.6}Ca_{0.4}MnO_{3-\delta}$. The $P(O_2)$ in the outlet gas is calculated from the EMF of the zirconia sensor. Using the gas flow rate and the calculated $P(O_2)$, the flux of oxygen is obtained. The difference in the flux of oxygen between the steady state and the transient state is attributed to the oxygen released or incorporated by $La_{0.6}Ca_{0.4}MnO_{3-\delta}$. By a graphical integration with time on this difference, the amounts of oxygen released and incorporated at the transient state after the polarization and after current interruption are obtained. Both values essentially agreed for respective runs. It is clear that the oxide electrode releases or incorporates oxygen with the change in the polarization.

Using the amount of $La_{0.6}Ca_{0.4}MnO_3$ applied to the cell, the amount of incorporated or released oxygen was converted to the change in oxygen nonstoichiometry of $La_{0.6}Ca_{0.4}MnO_3$ between the condition in equilibrium with the gas phase and that in a_O determined by E. The results are shown in Fig. 9. In Fig. 9, the $P(O_2)$ is calculated from E_{el}

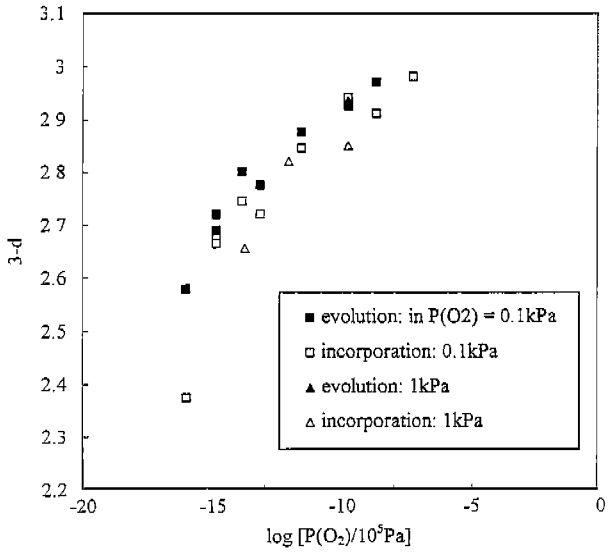

Fig. 9. Nonstoichiometry of $La_{0.6}Ca_{0.4}MnO_{3-\delta}$ at 800°C determined by the oxygen evolution and incorporation at the transient state cathodic polarization.

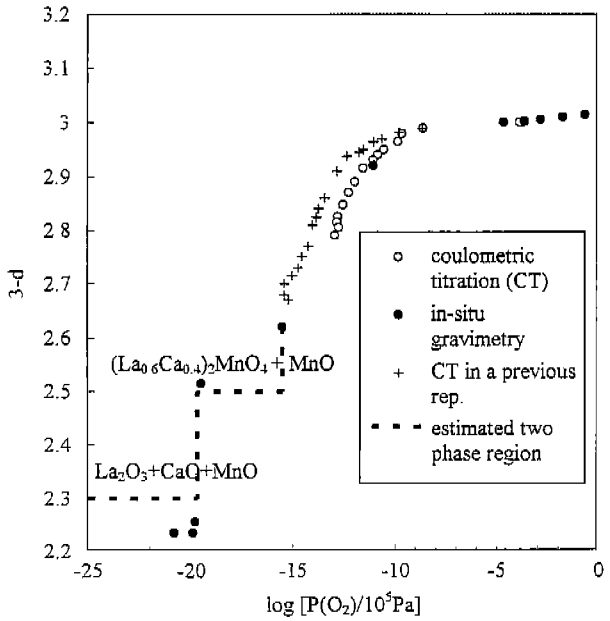

Fig. 10. Nonstoichiometry of $La_{0.6}Ca_{0.4}MnO_{3-\delta}$ at 800°C.

using the Nernst equation.

$$\log [P(O_2)/10^5 \text{ Pa}] = 4E_{el}F/RT \quad (9)$$

2. Nonstoichiometry Determined by the Coulometric Titration and High Temperature Gravimetry

Fig. 10 shows the results of nonstoichiometry measurements in the present work (circles) along with the date reported in the preceding paper[13] and proceedings[10,11] (daggers). In this work, nonstoichiometry is determined both by the high temperature gravimetry using Ar-O_2 and H_2-H_2O gas mixtures, as well as by the coulometric titration. Thus, the results are considered reliable. In the preceding work, we only used the coulometric titration. In the previous studies of the coulometric titration, gas leakage through the zirconia tubes was a big problem and we tried to compensate it by calculation. Comparing the two results in Fig. 10, the gas leakage seems to have been overestimated in the previous work. In the present study, we could not detect clear gas leakage. Since the present data was measured 6 years after the previous one, the improvement of commercial YSZ tube is considered as a major reason of the improvement of the data. Except for the absolute value, two sets of the data are similar.

Similar to $La_{0.6}Sr_{0.4}MnO_{3-\delta}$, $La_{0.6}Ca_{0.4}MnO_{3-\delta}$ is considered to decompose into $0.5(La_{0.6}Ca_{0.4})_2MnO_4$+0.5MnO at log $[P(O_2)/10^5$ Pa]=–15~–16. From the data of gravimetry (closed circles), $(La_{0.6}Ca_{0.4})_2MnO_4$ is considered to decomposes into La_2O_3, CaO and MnO at log $[P(O_2)/10^5$ Pa]<–20. The amount of stoichiometric oxygen expected from these decomposition is indicated in Fig. 10. The high-temperature gravimetry data well agree with the expected oxygen content. Nonstoichiometry in $La_{0.6}Ca_{0.4}MnO_{3-\delta}$ is very small at log $[P(O_2)/10^5$ Pa]>–10.

3. Nonstoichiometry and Oxygen Evolution/incorporation

In Fig. 11, the nonstoichiometry estimated from the electrochemical oxygen evolution and incorporation is compared with the one determined by coulometric titration and high temperature gravimetry. It should be noted that the oxygen potential in the cathode is calculated not by the gas phase $P(O_2)$ but by the potential at the $La_{0.6}Ca_{0.4}MnO_{3-\delta}$/YSZ interface, as indicated in Fig. 2 and by Eq. (9).

Since the two set of data agreed each other, the oxygen potential in $La_{0.6}Ca_{0.4}MnO_{3-\delta}$ cathode is exactly determined

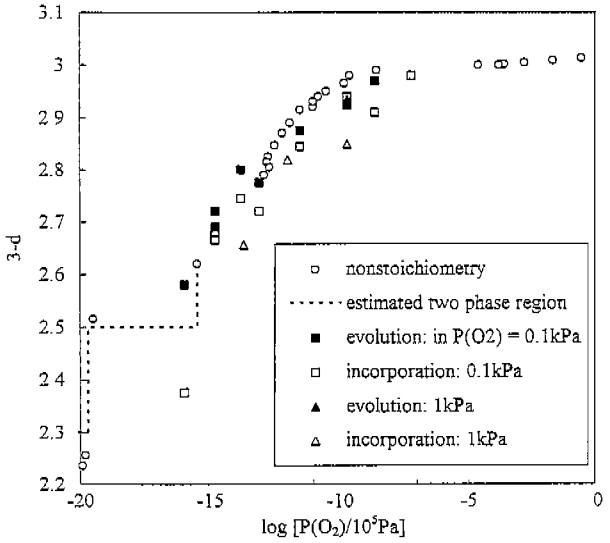

Fig. 11. Nonstoichiometry of $La_{0.6}Ca_{0.4}MnO_3$ estimated from the oxygen evolution and absorption under electrochemical transient state compared with that determined by the coulometric titration and high-temperature gravimetry.

by the potential at the $La_{0.6}Ca_{0.4}MnO_{3-\delta}$/YSZ interface and no remarkable potential gradient exists in the $La_{0.6}Ca_{0.4}MnO_{3-\delta}$ layer. That is, the potential profile is exactly the one corresponding to the surface reaction or the gas phase diffusion controlled kinetics in Fig. 2. This is consistent with the fact that the region where the oxygen evolution or incorporation by $La_{0.6}Ca_{0.4}MnO_{3-\delta}$ is remarkable overlaps the region where the limiting current is observed. Oxygen potential gradient should exists in $La_{0.6}Ca_{0.4}MnO_{3-\delta}$ layer when the surface or bulk diffusion controls the reaction rate. However, under such conditions, the overpotential is small and the oxygen potential is not low enough for the nonstoichiometry of $La_{0.6}Ca_{0.4}MnO_{3-\delta}$ large enough to release the observable amount of oxygen.

IV. Conclusion

1. When the electrochemical reaction takes place, the oxygen potential in $La_{0.6}Ca_{0.4}MnO_{3-\delta}$ (oxide cathode) deviates from that of the gas phase.

2. When the reaction is controlled by the gas phase diffusion, the oxygen potential in the oxide is determined by the potential at the oxide/YSZ interface.

References

1. J. Mizusaki, H. Tagawa, K. Tsuneyoshi, K. Mori and A. Sawata, "Electrode Thickness, Microstructure and Properties of Air Electrode for High-Temperature Solid Oxide Fuel Cells, $La_{0.6}Ca_{0.4}MnO_3$/YSZ," *J. Chem. Soc. Jpn. Chem. and Industrial Chem.*, **9**, 1623-1629 (1988).
2. J. Mizusaki, H. Tagawa, K. Tsuneyoshi and A. Sawata, "Reaction Kinetics and Microstructure of the Solid Oxide Fuel Cells Air Electrode $La_{0.6}Ca_{0.4}MnO_3$/YSZ," *J. Electrochem. Soc.*, **138**(7), 1867-1873 (1991).
3. K. Tsuneyoshi, K. Mori, A. Sawata, J. Mizusaki and H. Tagawa, "Kinetic Studies on the Electrode Reaction at the $La_{0.6}Ca_{0.4}MnO_3$/YSZ Interface, as an SOFC Air Electrode," *Solid State Ionics*, **35**, 263-268 (1989).
4. H. Kamata, A. Hosaka, J. Mizusaki and H. Tagawa, "Oxygen Reduction Behavior at Co-fired $La_{0.8}Sr_{0.2}MnO_3$/YSZ Interface, as an SOFC Air Electrode," *Denki Kagaku*, **66**(5), 407-413 (1997).
5. H. Kamata, A. Hosaka, J. Mizusaki and H. Tagawa, "High Temperature Electrocatalytic Properties of the SOFC Air Electrode $La_{0.8}Sr_{0.2}MnO_3$/YSZ," *Solid State Ionics*, **106**, 237-245 (1998).
6. J. Mizusaki, K. Amano, S. Yamauchi and K. Fueki, "Electrode Reaction at Pt, O_2(g)/Stabilized Zirconia Interfaces," *Solid State Ionics*, **22**, part I: 313-322, part II: 323-330 (1987).
7. A. Hammouche, E. Siebert, A. Hammou and M. Kleitz, "Electrocatalytic Properties and Nonstoichiometry of the High Temperature Air Electrode $La_{1-x}Sr_xMnO_3$," *J. Electrochem. Soc.*, **138**, 1212-1216 (1991).
8. J. Mizusaki, T. Saito and H. Tagawa, "A Chemical Diffusion-Controlled Electrode Reaction at the Compact $La_{1-x}Sr_xMnO_3$/Stabilized Zirconia Interface in Oxygen Atmospheres," *J. Electrochem. Soc.*, **143**(10), 3065-3073 (1996).
9. H. Tagawa, J. Mizusaki, H. Takai, Y. Yonemura, H. Minamiue and T. Hashimoto, "Oxygen Hyperstoichiometry in Perovskite-Type Oxide, Undoped and Sr-doped $LaMnO_3$," Proc. 17th Risø International Symp. Materials Sci., Roskilde, Denmark, pp. 437-442 (1996).
10. J. Mizusaki, H. Narita, H. Tagawa, M. Katoh and K. Hirano, "Anomalous Oxygen Evolution from Zirconia Cells at the Transient State," Proc. Science and Technology of Zirconia V, pp. 839-846 (1993).
11. J. Mizusaki, H. Tagawa, T. Saito and H. Narita, "Oxygen Reduction Kinetics at the Solid Oxide Fuel cell Air Electrode $La_{1-x}M_xMnO_3$ (M=Sr or Ca)/YSZ," Proc. 14th Risø International Symp. Materials Sci., Roskilde, Denmark, pp. 343-350 (1993).
12. H. Narita, J. Mizusaki and H. Tagawa, "Characteristic Impedance Spectrum Associated with Partial Reduction of Electrolyte and/or Electrode of Zirconia Cells," *Denki Kagaku*, **61**, 756-757 (1993).
13. J. Mizusaki, "Novel and/or Improved Experimental Techniques for the Studies of Bulk and Interfacial Properties of Solid Electrolytes," *Solid State Ionics*, **86-88**, 335-1342 (1996).
14. J. Mizusaki, H. Tagawa, K. Naraya and T. Sasamoto, "Nonstoichiometry and Thermochemical Stability of the Perovskite-type $La_{1-x}Sr_xMnO_{3-\delta}$," *Solid State Ionics*, **49**, 111-118 (1991).
15. J. Mizusaki, Y. Mima, S. Yamauchi, K. Fueki and H. Tagawa, "Nonstoichiometry of the Perovskite-type Oxides $La_{1-x}Sr_xCoO_{3-\delta}$," *J. Solid State Chem.*, **80**(1), 102-111 (1989).